Cooperative Localization in GNSS-aided VANETs with Accurate IR-UWB Range Measurements

G.M. Hoang[†‡], B. Denis[†], J. Härri[‡], D. T.M. Slock[‡]
[†]CEA-Leti, MINATEC Campus, 17 avenue des Martyrs, F38054 Grenoble, Cedex 9, France
[‡]EURECOM, 450 route des Chappes, 06904 Sophia Antipolis, France
E-mails:{giaminh.hoang, benoit.denis}@cea.fr, {jerome.haerri, dirk.slock}@eurecom.fr

***Abstract*—Cooperative localization based on Impulse Radio - Ultra WideBand (IR-UWB) is known to provide a centimeter-level ranging resolution when the anchor nodes have perfectly known positions. In Vehicular Ad-Hoc Networks (VANETs), vehicles acting as "virtual anchor" nodes are highly mobile with imperfect GNSS position estimates. The large difference between measurement noises of the (Global Navigation Satellite System) GNSS position and the IR-UWB (Vehicle-to-Vehicle) V2V ranging creates a bias in the localization filter, which is cooperatively propagated to other anchor nodes, and therefore significantly attenuates the benefits of IR-UWB for cooperative localization. This paper compensates this drawback by a novel 2-step cooperative localization fusion framework. It first selects the "virtual anchor" nodes with the lowest GNSS position uncertainty to mitigate and stop the propagation of the bias. Once all bias have been reduced, it refines the localization precision through exhaustive fusion between "virtual anchors". This strategy increases the probability to reach a 40 cm precision from 25% (conventional IR-UWB) to 95%, and even a 20cm precision from 5% to 40%.**

I. Introduction

Cooperative Intelligent Transport Systems (C-ITS) applications based on Vehicular Ad hoc NETworks (VANETs) assume the availability of a Global Navigation Satellite System (GNSS) to provide each vehicle with its geo-positioning. Although sufficient for Day-1 C-ITS applications (e.g. route navigation, road hazard warning, or networking…), the GNSS accuracy, reliability and availability are clearly not sufficient for Day-2 applications (e.g. Highly Autonomous Driving (HAD), safety of Vulnerable Road Users (VRU)…), which require a constant centimeter-level localization accuracy. Cooperative Localization (CLoc) is a promising strategy aiming at reaching such high localization accuracy.

Conceptually speaking, CLoc in a VANET context increases vehicles absolute geo-localization by considering their neighboring vehicles as potential "virtual anchors" (i.e. anchor with only approximate position knowledge). In this context, each vehicle piggybacks its absolute geo-localization in a "Beacon" sent over "V2X" technology[1]. Through the reception of these "Beacons", an "ego" vehicle becomes aware of the *absolute* position estimate of its neighbors, and use the 'Beacon' signal statistics to further sample *relative* position information (e.g. Vehicle-to-Vehicle (V2V) distances, relative angles…). It then performs ad hoc trilateration and fuses with its on-board GNSS position to enhance its own *absolute* geo-localization (See Fig. 1). This vehicle in turn improves the geo-localization of other vehicles by further broadcasting its enhanced position in "Beacons".

In literature, CLoc has already been applied in [1]–[3] to fuse on-board GNSS estimates with opportunistic V2V Received Signal Strength Indicators (RSSIs) out of "Beacons" called Cooperative Awareness Messages (CAMs) [4] sent on the V2X ITS-G5 technology[2]. The cooperative solution in [1] is based on a dissimilarity matrix composed of V2V RSSI measurements. The latter are injected as observations into an Extended Kalman Filter (EKF), while using GNSS estimates for initialization purposes only. In [2], [3], GNSS positions and V2V RSSI measurements are combined within a global EKF or Particle Filter (PF) framework, while compensating for asynchronous input data. A major advantage of using V2V RSSI is full compliance with future ITS-G5 connected vehicles[3]. Yet, V2V RSSI is also known to provide limited accuracy and reliability, especially in non-static multi-path environments, where channel parameters (i.e., path loss, reflection, shadowing…) fluctuate.

In this paper, we propose to replace the ITS-G5-based RSSI by Impulse Radio - Ultra WideBand (IR-UWB) Time-of-Flight (ToF). Compared to ITS-G5 RSSI, IR-UWB ToF is known to provide centimer-level distance resolutions. Our approach combines local on-board GNSS positions, neighboring GNSS positions sent over ITS-G5 technology, and ToF ranging from IR-UWB in a PF framework. Although similar ideas were presented in [5], [6], they are limited to general wireless sensor networks, not considering potential low GNSS neighboring estimates from moving vehicles. Our contributions are threefold: (i) we illustrate the bias created and propagated by CLoc strategies when fusing two types of estimates with strongly different uncertainties (e.g. GNSS and IR-UWB ToF); (ii) we propose a two-step CLoc strategy to mitigate such bias, selecting first the best "virtual anchors" with lowest GNSS uncertainties to break the propagation of the bias, then exhaustively fusing estimates from other neighbors, once the bias has been mitigated; (iii) we compare

[1]To remain technology neutral, a "Beacon" is a message periodically broadcast by each node, while "V2X" (Vehicle-to-X) refers to any technology capable of Device-to-Device (D2D) communication.

[2]CAM and ITS-G5 are European counterparts to the Basic Safety Message (BSM) and Dedicated Short Range Communication (DSRC) in the US.

[3]ITS-G5 is expected to be available in every vehicle sold from 2019.

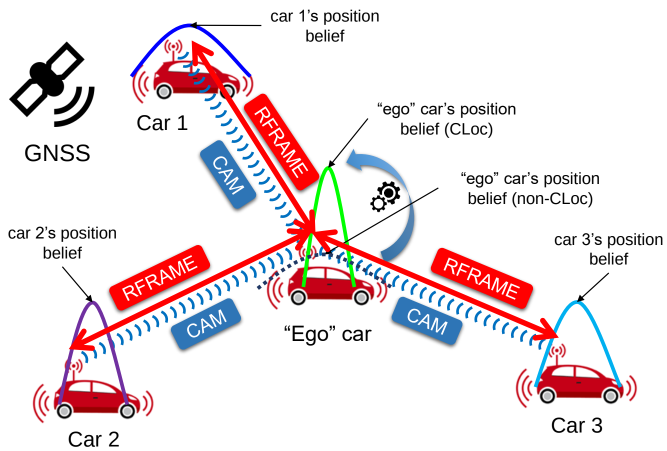

Fig. 1. "Ego" car receiving CAMs and exchanging ranging frames RFRAME from/with single-hop "virtual anchors" to perform distributed CLoc. The CLoc position beliefs (i.e. through fused GNSS and ITS-G5 RSSIs/IR-UWB ranges) are expected to be more concentrated than the non-CLoc position beliefs (i.e., standalone GNSS).

our strategy against various benchmarks and illustrate our superior performance.

The paper is organized as follows. In Section II, we formulate the CLoc problem. In Section III, we describe the specific issues related to IR-UWB measurements and introduce the 2-step CLoc scheme. In Section IV, comparative simulation results are presented. Finally, Section V concludes the paper and provides an outlook of remaining challenges.

II. General Problem Formulation

A. Cooperative Localization in VANETs

We consider here a set of cooperative GNSS-equipped vehicles exchanging CAMs over ITS-G5 technology. In addition, these vehicles are also endowed with IR-UWB ranging capabilities. The goal of an "ego" vehicle is to infer its position (as part of its so-called "state" in the following) based on its own estimated GNSS position, on V2V IR-UWB ranges with respect to 1-hop neighbors, and on imperfect state information from these neighbors, viewed as "virtual" anchors (i.e., estimated locations and their related uncertainties, encapsulated in the CAMs). Fig. 1 illustrates the CLoc concept. We do not consider V2I communications here to assist positioning, even though Road Side Units (RSU) could be helpful (e.g., ITS-G5 or WiFi access points (APs) in most urban environments). Our aim is to remain independent from any additional infrastructure (i.e., other than the GNSS infrastructure itself), which not only significantly reduces deployment costs but also operates seamlessly in infrastructure-less roads.

B. Overall System Model

We first define the state vector $\boldsymbol{\theta}_{i,k} = [\mathbf{x}_{i,k}^\dagger, \mathbf{v}_{i,k}^\dagger]^\dagger$ of vehicle i including, for a 2-D system, its position $\mathbf{x}_{i,k} = [x_{i,k}, y_{i,k}]^\dagger$ and its velocity $\mathbf{v}_{i,k} = [v_{i,k}^x, v_{i,k}^y]^\dagger$ at discrete time step k[4] according to its local timeline. In the following, we describe the models for vehicle localization and tracking.

1) Mobility Model: We consider a stochastic mobility model suitable to vehicular contexts, referred to as the modified Gauss-Markov mobility model [3], as follow:

$$\boldsymbol{\theta}_{i,k+1} = \begin{bmatrix} \mathbf{I}_2 & \alpha\Delta T\cdot\mathbf{I}_2 \\ \mathbf{0}_2 & \alpha\cdot\mathbf{I}_2 \end{bmatrix}\boldsymbol{\theta}_{i,k} + (1-\alpha)\begin{bmatrix}\Delta T\cdot\mathbf{I}_2 \\ \mathbf{I}_2\end{bmatrix}\bar{\mathbf{v}}_i + \sqrt{1-\alpha^2}\begin{bmatrix}\Delta T^2\cdot\mathbf{I}_2 \\ \Delta T\cdot\mathbf{I}_2\end{bmatrix}\mathbf{w}_{i,k}, \tag{1}$$

where α is the memory level, ΔT the time step, $\bar{\mathbf{v}}_i = [v_i^x, v_i^y]^\dagger$ the asymptotic 2-D velocity, $\mathbf{w}_{i,k} = [w_{i,k}^x, w_{i,k}^y]^\dagger$ the 2-D process noise vector, $\mathbf{I}_2$ the identity matrix of size 2×2. Note that we use this mobility model to perform the prediction of both "ego" and neighbors' estimated locations and resynchronize related data before fusion, like in [2], [3].

2) Observation Model: This paper considers two different measurements, which are interdependently produced by a GNSS receiver and an IR-UWB transceiver respectively.

a) GNSS Absolute Position: The 2-D estimated GNSS position, $\mathbf{x}_{i,k}^{\text{GNSS}} = [z_{i,k}^x, z_{i,k}^y]^\dagger$, is affected by an additive noise term $\mathbf{n}_{i,k}^{\text{GNSS}} = [n_{i,k}^x, n_{i,k}^y]^\dagger$, which is assumed to be i.i.d. centered Gaussian [2], [3], [7], as follows:

$$z_{i,k}^x = x_{i,k} + n_{i,k}^x, \quad z_{i,k}^y = y_{i,k} + n_{i,k}^y. \tag{2}$$

b) IR-UWB V2V Ranges: Through a cooperative ranging protocol (e.g., based on the Time of Arrival (ToA) estimation of transmitted packets involved in multiple-way handshake transactions [8] , node i can estimate the V2V distance $z_{j\to i,k}$ with respect to node j:

$$z_{j\to i,k} = \|\mathbf{x}_{i,k} - \mathbf{x}_{j,k_i}\| + n_{j\to i,k}, \tag{3}$$

where $n_{j\to i,k}$ is an i.i.d. centered Gaussian noise term with standard deviation σ_{UWB}.

In the following fusion filtering scheme, input observations can be composed of GNSS and/or UWB range measurements, depending on the cooperation level. Generally, given the set $\mathcal{S}_{\to i,k}$ of vehicle i's neighbors used as "virtual anchors" at time k_i, the full measurement vector is $\mathbf{z}_{i,k} = [z_{i,k}^x, z_{i,k}^y, \ldots, z_{j\to i,k}, \ldots]^\dagger$, $j \in \mathcal{S}_{\to i,k}$.

C. Fusion Particle Filter

The key idea of Particle Filters (PF) is to approximately represent the *a posteriori* density $p(\boldsymbol{\theta}_{i,k}|\mathbf{z}_{1:k})$ by a particle cloud $\{\boldsymbol{\theta}_{i,k}^{(p)}, w_{i,k}^{(p)}\}_{p=1}^P$ of random samples $\boldsymbol{\theta}_{i,k}^{(p)}$ with associated weights $w_{i,k}^{(p)}$, and to compute a state estimate (e.g., according to the Minimum Mean Square Error (MMSE) estimator) based on these samples and weights. At time step k_i, the PF recursively updates the previous particle cloud $\{\boldsymbol{\theta}_{i,k-1}^{(p)}, w_{i,k-1}^{(p)}\}_{p=1}^P$ using the observation $\mathbf{z}_{i,k}$ by doing prediction step (i.e., approximating the predicted *posterior* $p(\boldsymbol{\theta}_{i,k}|\mathbf{z}_{i,1:k-1})$) and

[4] Due to asynchronously sampled time instants, the index k is different from one vehicle to others. The subscript of the "ego" vehicle is dropped for notation brevity.

correction step (i.e., computing these weights $w_{i,k}^{(p)}$ relying on the likelihood function given current observations, $p(\mathbf{z}_{i,k}|\boldsymbol{\theta}_{i,k},\ldots,\boldsymbol{\theta}_{j,k_i},\ldots)$, $j \in \mathcal{S}_{\rightarrow i,k}$). We then propose to apply the PF described in Algorithm 1 as the core filter/fusion engine of our CLoc framework. Several variants aiming at reducing V2V channel congestion and CAM overhead (e.g., through simplified cloud representation) are also proposed in [9].

Algorithm 1 Bayesian bootstrap (iteration k, "ego" vehicle i)

1: receive CAMs from the set $\mathcal{N}_{\rightarrow i,k}$ of perceived neighboring vehicles, read the RSSI values (optional), and extract the neighboring particle clouds $\boldsymbol{\theta}_{j,k^*}^{(p)}$, $p = 1 \ldots P$, $j \in \mathcal{N}_{\rightarrow i,k}$

2: perform prediction/data resynchronization at the "ego" estimation instance k (i.e., the global time $t_{i,k}$)

$$\begin{aligned} \boldsymbol{\theta}_{j,k_i}^{(p)} &\sim p\left(\boldsymbol{\theta}_{j,k_i}\middle|\boldsymbol{\theta}_{j,k^*}^{(p)}\right), && j \in \{i\} \cup \mathcal{N}_{\rightarrow i,k}, \\ w_{j,k|k-1}^{(p)} &= w_{j,k-1}^{(p)} = 1/P, && p = 1,\ldots,P, \end{aligned}$$

and build the local dynamic map (LDM) of vehicle i's neighbors as the first output

$$\hat{\boldsymbol{\theta}}_{j,k_i} \approx \sum_{p=1}^{P} w_{j,k|k-1}^{(p)} \boldsymbol{\theta}_{j,k_i}^{(p)} = \frac{1}{P}\sum_{p=1}^{P} \boldsymbol{\theta}_{j,k_i}^{(p)}, \quad j \in \mathcal{N}_{\rightarrow i,k}$$

3: check the ranging protocol to access the available IR-UWB ranges to the set $\mathcal{S}_{\rightarrow i,k}$ of "virtual anchors" in its UWB piconet, manipulating the measurement and the corresponding observation model

$$\mathbf{z}_{i,k} = \begin{cases} \left[z_{i,k}^x, z_{i,k}^y\right]^\dagger, & \text{if non-fusion instant } k, \\ \left[z_{i,k}^x, z_{i,k}^y, \ldots, z_{j\rightarrow i,k}, \ldots\right]^\dagger, & \text{if fusion instant } k, \end{cases}$$

4: update new weights according to the likelihood based on

$$w_{i,k}^{(p)} \propto p\left(\mathbf{z}_{i,k}\,\middle|\,\boldsymbol{\theta}_{i,k}^{(p)},\ldots,\boldsymbol{\theta}_{j,k_i}^{(p)},\ldots\right), \quad p = 1,\ldots,P,$$

normalize them to sum to unity, and compute the approximate mean as the second filter/fusion output

$$\hat{\boldsymbol{\theta}}_{i,k} \approx \sum_{p=1}^{P} w_{i,k}^{(p)} \boldsymbol{\theta}_{i,k}^{(p)}$$

5: perform resampling and broadcast

III. IR-UWB-BASED COOPERATIVE LOCALIZATION

A. IR-UWB Range Accuracy vs. "Anchors" Uncertainty

In our data fusion framework described in Sec. II-B, two modalities are used, namely the estimated positions (i.e., that of both "ego" and neighboring vehicles) and IR-UWB range measurements with respect to neighboring vehicles. The filter naturally weights these modalities according to their uncertainties (i.e., relying on *a priori* covariance matrices).

The challenge behind IR-UWB cooperative localization is related to the largely different levels of uncertainty between these two modalities, i.e. the uncertainty of IR-UWB ranging is rather small in comparison with that of the predicted position (from GNSS, position prediction/resynchronization, out-of-date CAMs...). Would these two modalities be uncorrelated, the filter would easily reject the outlier. However, these two modalities are strongly correlated, as the IR-UWB ranging is only valid as function of the estimated position of the sender. Accordingly, the filter will be influenced by the large uncertainty and loose its correction power, as conceptually illustrated on Fig. 2. We first consider on Fig. 2(a) the case where both modalities have similar levels of uncertainty (belief). When the ego vehicle receives the predicted position and the IR-UWB ranging estimates, the filter manages to reduce its own position uncertainty (i.e. red bold circle from orange circle). But when the predicted position of the neighbor includes a large bias, the IR-UWB in turn becomes strongly biased and actually increases the uncertainty (belief) of the estimated ego position and shift it further away from the true position, as depicted as a bold red circle on Fig. 2(b).

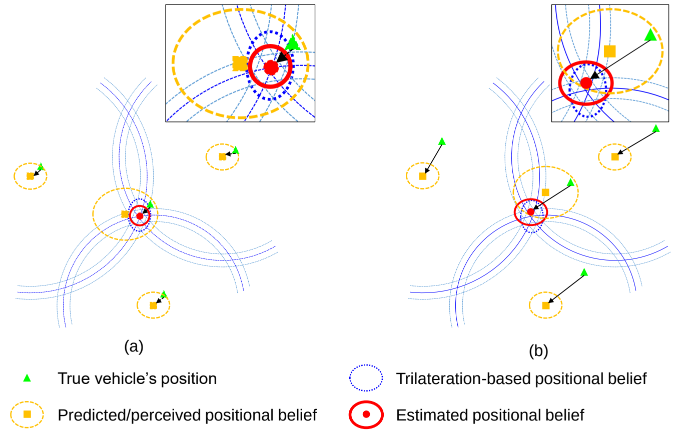

Fig. 2. Simplified illustration of the effect of biased positions of "virtual anchors" on "ego" filter correction with high-accuracy IR-UWB range measurements.

Selecting the right "virtual" anchors is therefore critical in IR-UWB cooperative localization, as each vehicle in turn will cooperatively participate to the localization process, further propagating its uncertainty and as such impacting the uncertainty of its neighboring vehicles.

B. Two-Step Cooperative Localization Strategy

So as to cope with the previous harmful phenomena, we propose a two-step CLoc procedure.

1) Bias mitigation step: This first step, called "bias mitigation", let each vehicle selectively cooperates with neighbors that have the presumably best estimated positions. This is achieved by encapsulating the confidence level of estimated position (e.g. GNSS position covariance matrix) either in CAMs or in dedicated IR-UWB ranging packets. The Bayesian Cramér-Rao Lower Bound (BCRLB)-based link selection proposed in [3] is a potential strategy to the Bias mitigation step. However, this solution cannot handle the case, where neighbors' position beliefs can be very concentrated but strongly biased. A BCRLB-based link selection accounting only for the variance will fail to remove the biased position estimates of the "virtual" anchors. The approach followed here is to to let vehicles equipped with high-class GNSS receivers (e.g., RTK, PPP. . .) inform their neighbors about their high reliability (i.e., through CAMs). Accordingly, neighboring vehicles may rely on this information to avoid biased "virtual" anchors.

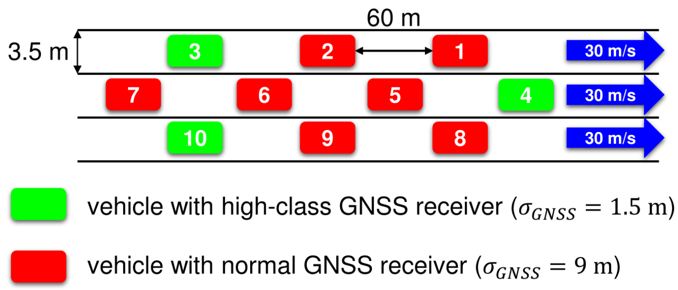

Fig. 3. Constellation of the evaluated VANETs and heterogeneous GNSS configuration in highway scenario.

Then after a few iterations, by integrating only contributions from presumably bias-free neighbors and thus by avoiding bias propagation, all vehicles in the proximity will have significantly reduced their own possible bias.

2) Accuracy refinement step: When the biases in the position estimates of the "virtual" anchors are alleviated, one can then benefit from them as accurately localized neighbors. In other word, exhaustive CLoc is preferred in this so-called "accuracy refinement" step to boost the localization accuracy to the fullest.

IV. Simulation Results

We model a common 3-lane highway, where 10 ITS-G5 connected vehicles endowed with IR-UWB ranging capabilities[5] are driving steadily in a common direction at the average speed of 110 km/h (i.e., ≈ 30 m/s) for 60 seconds, as shown in Fig. 3. In this paper, we consider a realistic heterogeneous scenario where vehicles have the same visibility to the satellite constellation, but suffer from disperse and independent GNSS levels due to different receiver capability (e.g., RTK, PPP vs. basic receivers)[6] as in [3] (See Fig. 3). We implemented the 2-step fusion framework described in Sec. II-B and Sec. III on Matlab, where most relevant simulation parameters are summarized in Table I, and the the different tested algorithm are specified in Table II.

TABLE I
Main simulation parameters.

Parameter	Value
Memory level α	0.95
Tangential acc. uncertainty	1 [m/s^2]
Perpendicular acc. uncertainty	0.1 [m/s^2] (to satisfy road constraints)
Sampling period ΔT	0.1 [s]
Std. of GNSS x- or y-errors	1.5 [m] (non-degraded), 9 [m] (degraded)
GNSS rate	10 [Hz]
CAM rate	10 [Hz] (critical)
Std. of UWB ranging noise	0.2 [m]
Number of particles	1,000

TABLE II
Description of different UWB CLoc schemes

Scheme	Degraded GNSS node	Non-degraded GNSS node
Conventional CLoc	Exhaust. CLoc	Exhaust. CLoc
2-step semi-CLoc	Select. CLoc (first) Exhaust. CLoc (second)	Non-CLoc (all)
2-step full-CLoc	Select. CLoc (first) Exhaust. CLoc (second)	Non-CLoc (first) Exhaust. CLoc (second)

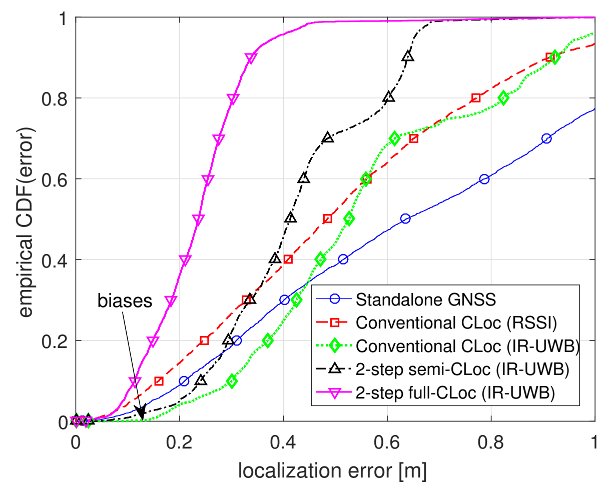

Fig. 4. Empirical CDF of localization errors considering degraded GNSS for different schemes w.r.t. fused modalities and CLoc techniques.

A. Results

Fig. 4 and Fig. 5 compare the localization performance at degraded GNSS vehicles in terms of empirical Cumulative Density Functions (CDFs) and Root Mean Square Errors (RMSEs) respectively, whereas Fig. 6 shows similar comparison at non-degraded GNSS ones by means of empirical CDFs. As expected and in accord with previous studies from [2], [3], [9], [10], the fusion of several modalities (e.g., on-board GNSS position and ITS-G5 RSSIs/IR-UWB ranges) yields localization accuracy gain comparing with the standalone solutions (e.g., GNSS). Nevertheless, one expects that the highly accurate IR-UWB ranges would considerably boost the localization accuracy beyond what unreliable RSSIs could give. However, as shown in the three figures (e.g., Fig. 4, 5, and 6), when being associated with conventional CLoc, the fused GNSS+IR-UWB only provides comparable accuracy with the combined GNSS+RSSI. The biased "virtual" anchors strongly impact the conventional fusion of GNSS position and IR-UWB ranges. Under degraded GNSS vehicles, it does not produces any accuracy gain compared to GNSS+RSSI, while in non-degraded GNSS vehicles, only modest improvements are observed. This can be explained as follows. Our PF fuses three source of information i.e., the predicted position, the

[5]We leave the investigation of a partial penetration of IR-UWB to future work.

[6]We leave the investigation of a heterogeneous visibility to satellite constellation to future work.

TABLE III
OVERALL PERFORMANCE COMPARISON OF DIFFERENT LOCALIZATION SCHEMES

Scheme	Degraded GNSS vehicles					Non-degraded GNSS vehicles[a]				
	Med. [m]	WC [m]	$P(0.2\ m)$	$P(0.4\ m)$	Acc. gain[b]	Med. [m]	WC [m]	$P(0.2\ m)$	$P(0.4\ m)$	Acc. gain[b]
Standalone GNSS	0.63	1.27	8.9%	29.9%	–	0.22	0.43	46.6%	86.0%	–
Conv. CLoc (RSSI)	0.48	0.91	14.4%	38.8%	23.8%	0.20	0.42	49.1%	87.7%	9.1%
Conv. CLoc (IR-UWB)	0.53	0.92	4.0%	24.8%	15.9%	0.23	0.37	42.6%	94.8%	-4.5%
2-step semi-CLoc (IR-UWB)	0.41	0.64	5.1%	45.7%	34.9%	0.22	0.43	46.6%	86.0%	0.0%
2-step full-CLoc (IR-UWB)	0.24	0.34	36.17%	95.7%	61.9%	0.18	0.29	57.7%	99.7%	18.2%

[a] Remind that non-degraded GNSS vehicles do not cooperate in the 2-step semi-CLoc, hence, the accuracy performance is the same as that of the standalone filtered GNSS approach.
[b] Accuracy gain (negative value in case of degradation) w.r.t. standalone filtered GNSS solution in median error (i.e., CDF = 50%).

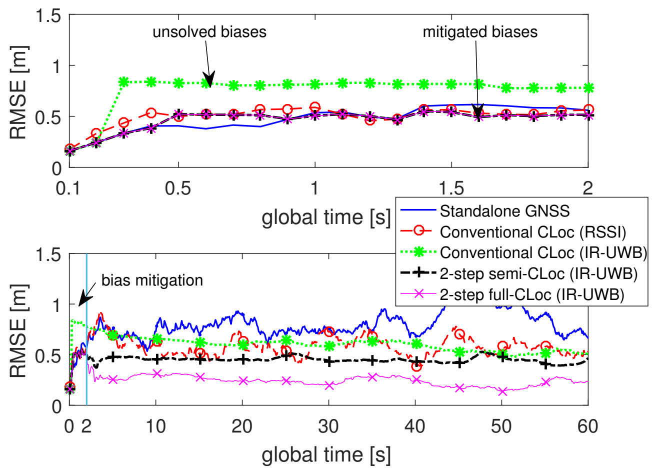

Fig. 5. Localization RMSE considering degraded GNSS as a function of time for different schemes w.r.t. fused modalities and CLoc techniques.

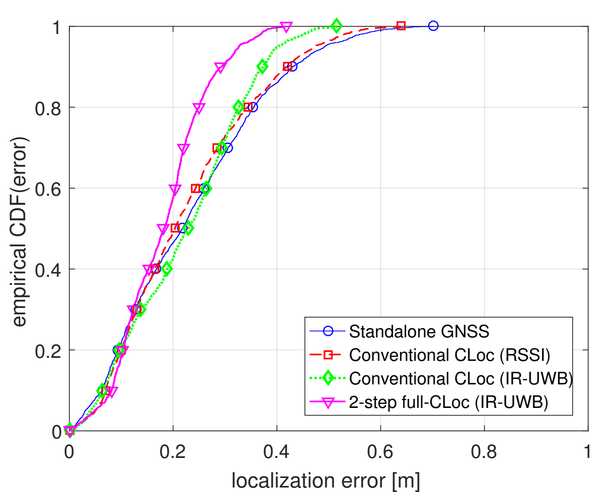

Fig. 6. Empirical CDF of localization errors considering non-degraded GNSS for different schemes w.r.t. fused modalities and CLoc techniques.

GNSS positions, and the distance information to the imperfect "virtual" anchors. The PF is tricked to put more confidence on the UWB-based trilateration due to the small ranging noise variance in the observation model. Accordingly, when integrating the biased localized neighbors, the fused position estimates also become biased. Furthermore, a closer look at Fig. 5 (bottom) reveals that the trend in RMSE of the two standalone GNSS and GNSS+RSSIs schemes are rather similar, but are different from the GNSS+IR-UWB ranges solution. It means the filter looks at the large RSSI noise variance in the observation model, then decides to use these RSSIs as an assistant modality after the predicted and GNSS positions. In contrast, accurate IR-UWB ranges make the filter mainly rely on them, therefore, the trend in the curves of UWB-based CLoc approaches are different from that of GNSS scheme. In case of non-degraded GNSS (See Fig. 6), the bias effect does not seem to be severe. In this case, the GNSS uncertainty is concentrated so the filer gives higher weight to the GNSS estimate. Accordingly, it is able to correct the bias caused by the trilateration procedure. However, the performance gain is limited due to the same cause previously described.

When employing the proposed 2-step CLoc, we observe that when the biases in position estimates of the vehicles are mitigated in the first step (See Fig. 5 (top)), the fused GNSS+IR-UWB then yields to remarkable performance in the "accuracy refinement" phrase. In particular, we observe in Fig. 5 (top) that in spite of good initialization, conventional GNSS+UWB ranges scheme performing exhaustive fusion gets biased after only 3 iterations, then converges to inaccurate values and give large confidence to them. The proposed CLoc, however, waits until all vehicles' position estimates are improved by the bias refinement phase, then boosts the performance by the exhaustive fusion phase. Between the semi-CLoc and full-CLoc, we obviously show that the latter solution is more effective and gives excellent accuracy. This can be explained as non-degraded GNSS vehicles can also improve their position estimates by cooperating with degraded GNSS ones after the mitigation step, and because degraded GNSS nodes benefit more by cooperating with more accurate ones. Finally, Table III summarizes the overall performance comparison. We show the probability to reach a 20 cm and 40 cm position accuracy in the case of degraded and non degraded GNSS. Next to it, we provide the accuracy gain, w.r.t the baseline standalone GNSS. We draw the attention that the CLoc approach proposed in this paper provides a 40 cm position accuracy (almost reaching 100% probability) in both degraded and non-degraded GNSS. It even manages to provide a 20 cm position accuracy with 36% and 57% probability for degraded and non degraded GNSS respectively. This is a straight 61% and 18% accuracy gain in degraded and non-degraded GNSS respectively.

V. Conclusion

Cooperative Localization (CLoc) based on V2V Impulse Radio - Ultra Wide Band (IR-UWB) range estimates is a powerful strategy to increase up to a centimeter level the precision of the absolute positions of future connected vehicles. However, CLoc ends up being inefficient when fusing measurements with strongly different uncertainties, which is typically the case when fusing GNSS position estimates with IR-UWB ranging estimates. We proposed in this paper a novel 2-step CLoc strategy specifically targeted at mitigating this issue.

We illustrated how a bias is created by the GNSS large uncertainties on the IR-UWB estimates, which is then further propagated to other vehicles via cooperative position exchanges. Our 2-Step strategy prevents bias propagation by selectively using the best neighbors in the first step, then cooperating with all neighbors to boost the localization accuracy in the second step. This approach managed to provide a 40 cm geo-localization precision with 95% probability (compared to 25% for GNSS+IR-UWB), and even a 20 cm precision up to 36% probability (against 4% for GNSS+IR-UWB).

Future works will consider how to estimate the biases in order to capture the worst-case situation when all vehicles are poorly localized (e.g., in urban canyons or tunnels). It will also attempt to estimate the threshold between heterogeneous uncertainties, above which the bias start penalizing CLoc.

Acknowledgment

This work has been performed in the frame of the *HIGHTS* project, which is funded by the European Commission (636537-H2020). EURECOM acknowledges the support of its industrial members, namely, BMW Group, IABG, Monaco Telecom, Orange, SAP, ST Microelectronics, and Symantec.

References

[1] R. Parker and S. Valaee, “Vehicular node localization using received-signal-strength indicator,” *IEEE Trans. on Veh. Technol.*, vol. 56, pp. 3371–3380, Nov. 2007.

[2] G. M. Hoang, B. Denis, J. Härri, and D. T. M. Slock, “Distributed link selection and data fusion for cooperative positioning in GPS-aided IEEE 802.11p VANETs,” in *Proc. WPNC’15*, Mar. 2015.

[3] G. M. Hoang, B. Denis, J. Härri, and D. T. M. Slock, “Select thy neighbors: Low complexity link selection for high precision cooperative vehicular localization,” in *Proc. VNC’15*, Dec. 2015.

[4] “Intelligent Transport Systems (ITS); Vehicular Communications; Basic Set of Applications; Part 2: Specification of Cooperative Awareness Basic Service,” *ETSI Std. EN 302 637-2 V1.3.2*, Oct. 2014.

[5] H. Wymeersch, J. Lien, and M. Win, “Cooperative localization in wireless networks,” *Proc. of the IEEE*, vol. 97, pp. 427–450, Feb. 2009.

[6] K. Das and H. Wymeersch, “Censoring for Bayesian cooperative positioning in dense wireless networks,” *IEEE JSAC*, vol. 30, pp. 1835–1842, Oct. 2012.

[7] N. Drawil and O. Basir, “Intervehicle-communication-assisted localization,” *IEEE Trans. on Intel. Transp. Syst.*, vol. 11, pp. 678–691, Sept. 2010.

[8] M. Maman, B. Denis, M. Pezzin, B. Piaget, and L. Ouvry, “Synergetic MAC and higher layers functionalities for UWB LDR-LT wireless networks,” in *Proc. ICUWB’08*, vol. 3, pp. 101–104, Sept. 2008.

[9] G. M. Hoang, B. Denis, J. Härri, and D. T. M. Slock, “On communication aspects of particle-based cooperative positioning in GPS-aided VANETs,” in *Proc. CCP IV’16*, Jun. 2016.

[10] G. M. Hoang, B. Denis, J. Härri, and D. T. M. Slock, “Breaking the gridlock of spatial correlation in GPS-aided IEEE 802.11p-based cooperative positioning.” *accepted by IEEE Trans. on Veh. Technol.*, Jun. 2016.